mediated metabolic tumor effects using in vivo achievable biguanide concentrations.
Materials and Methods: Initially we developed ^{11}C labeled MET, which allowed assessment of in vitro cellular drug uptake and, importantly, in vivo biodistribution assessment using PET scans or organ dissection in tumor-bearing mice. Based on those results cellular effects of physiologically relevant doses of biguanides were tested in 14 cell lines using assays of proliferation/viability, glucose metabolism (FDG retention), respiration and lactic acid production (extracellular flux analyzer) and stress signaling. Finally, the two tumor models SiHa (cervix) and A549 (lung) were established in mice to assess acute and long-term metabolic, microenvironmental and anti-proliferative effects of PHEN treatment.
Results: In vivo results showed that [MET] in blood peaked at 250 µM in mice administered maximum tolerable dose (250 mg/kg). Furthermore, MET was retained by tumor cells in vitro as well as in vivo, and uptake could be blocked by unlabeled MET suggesting involvement of OCTs. MET uptake varied widely among cell lines, with the highest uptake in A549. Likewise, inhibition of respiration and stimulation of glucose use and cell viability/proliferation was mostly affected in cell lines with high MET uptake. Even so, most cell lines were insensitive to in vivo achievable MET concentrations. PHEN was 100 times more potent than MET and induced profound metabolic changes at 50 µM in all cell lines, and down to a physiological relevant concentration of 1 µM in A549. In accordance, PHEN was chosen for further testing in tumor-bearing mice. Data analysis of tumor microenvironment (hypoxia) and growth is ongoing.
Conclusions: Biguanides affect cellular energy metabolism and proliferation in vitro but metabolic effects of MET were typically restricted to non-physiological concentrations and MET retention and sensitivity varied significantly among cell lines. PHEN exerted similar effects as MET but with greater potency and may affect a broader selection of tumors at physiologically achievable concentrations. Labeling of biguanides may allow PET-based identification of patients with treatment-responsive tumors.

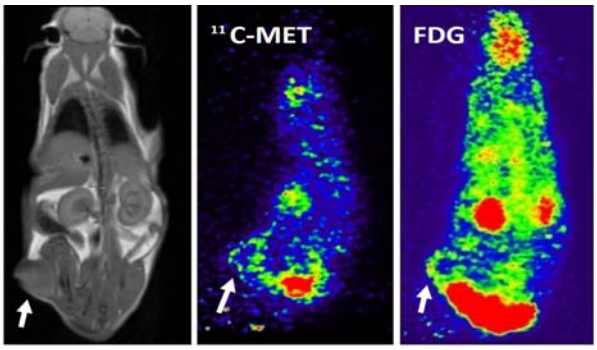

A549 tumor bearing mice were successively PET/MR scanned. White arrow marks tumor.

OC-0543

Carbon ion irradiation response depends less on tumor heterogeneity: RBE-comparison for 3 prostate tumor sublines

C. Glowa[1], P. Peschke[2], S. Brons[3], M. Scholz[4], J. Debus[1], C.P. Karger[5]
[1]*University Hospital Heidelberg, Clinical Radiology, Heidelberg, Germany*
[2]*German Cancer Research Center (DKFZ), Clinical Cooperation Unit Molecular Radiooncology, Heidelberg, Germany*
[3]*HIT, Heidelberg Ion Beam Therapy Center, Heidelberg, Germany*
[4]*Helmholtz Center for Heavy Ion Research (GSI), Biophysics, Darmstadt, Germany*
[5]*German Cancer Research Center (DKFZ), Medical Physics in Radiotherapy, Heidelberg, Germany*

Purpose/Objective: Carbon ions (^{12}C-ions) show an increased relative biological effectiveness (RBE) relative to photons. To compare the impact of intra- and intertumor heterogeneity on the RBE, dose-response curves for photons and ^{12}C-ions were determined for three sublines of a syngeneic rat prostate adenocarcinoma.
Materials and Methods: Fresh tumor fragments from three sublines (AT1, HI and H) of the Dunning prostate tumor R3327 were transplanted subcutaneously into the distal right thigh of male Copenhagen rats. Tumors were treated once with increasing single doses of either ^{12}C-ions or 6 MeV photons. Primary endpoint was local tumor control within 300 days. For the H-tumor, histological tumor control, defined as absence of proliferation (BrdU-injection) in the remaining fibrotic nodules (Hematoxylin/Eosin staining) was used as secondary endpoint. RBE-values were calculated by the ratio of TCD_{50}-values (dose to achieve 50% tumor control probability) for photons and ^{12}C-ions, respectively.
Results: Local tumor control can be achieved with ^{12}C-ions and photons in all three sublines. For all tumors an increased effectiveness of ^{12}C-ions was observed. The RBE for local tumor control increased from 1.62 ± 0.11 (H) to 2.08 ± 0.13 (HI) to 2.30 ± 0.08 (AT1). Using histological tumor control, the RBE for the H-tumor increased to 1.80 ± 0.13. For ^{12}C-ion irradiations the variation of TCD_{50}-values between tumor sublines was significantly smaller than after photon irradiation. Additionally ^{12}C-ion dose-response curves were much steeper compared to photons indicating a smaller intratumor heterogeneity for ^{12}C-ions.
Conclusions: The study confirms the increased relative biological effectiveness of ^{12}C-ions in tumors, which is the highest for the highly radioresistant AT1-tumor and the smallest for the well-differentiated H-tumor. The very heterogeneous moderately differentiated HI-tumor lies in between. This indicates a clear correlation between decreasing differentiation status and increasing RBE. ^{12}C-ions may therefore be beneficial especially in undifferentiated tumors, with a high photon resistance. Changes of RBE with tumor differentiation were predominantly caused by changes in the photon response. This supports the assumption that the response to ^{12}C-ions is less dependent on tumor heterogeneity compared to photons. Thus heterogeneities within patient populations or the existence of radioresistant subpopulations within single tumors may be expected to have less impact on the ^{12}C-ions radiation response. The underlying differential mechanisms are currently analyzed in ongoing histological and functional experiments.

OC-0544

Does the effect of depletion of mtDNA on radiotherapy response depend on the metabolic profile of the cell line?

M.W. Van Gisbergen[1], A.M. Voets[2], R.F. Hoffmann[3], R. Biemans[1], H.J.M. Smeets[2], L. Dubois[1], P. Lambin[1]
[1]*Maastricht University, Radiation Oncology, Maastricht, The Netherlands*
[2]*Maastricht University, Genetics and Cell Biology, Maastricht, The Netherlands*
[3]*University of Groningen, European Research Institute for the Biology of Ageing, Groningen, The Netherlands*

Purpose/Objective: For several years evidence is accumulating that not only the more eminent known nuclear DNA mutations but also different variations (e.g. deletions and mutations) in the mitochondrial DNA (mtDNA) are associated with a wide variety of cancers. Unlike nuclear DNA (nDNA), mtDNA is polyploid, only maternally inherited and is encoding for 13 subunits of the oxidative phosphorylation (OXPHOS) machinery responsible for aerobic ATP production. Several mutations and variations in genes involved in OXPHOS are associated with a decreased ATP production and increased oxidative stress. Current study aimed at characterizing proliferation, metabolism and intrinsic radiosensitivity in ρ^0 cells, cell lines depleted from their mtDNA. We hypothesized that ρ^0 cells have a pronounced glycolytic profile resulting in radiosensitization compared to their parental counterparts.
Materials and Methods: ρ^0 cells were generated by depleting BEAS-2B (lung/bronchus epithelial) immortalized cells or A549 (lung adenocarcinoma) and 143B (osteosarcoma) tumor cell lines from their mtDNA by adding ethidium bromide (50 ng/ml) to the culture media for several weeks. mtDNA copy number was checked by qPCR. Proliferation was assessed using the IncuCyte FLR and metabolic profiles (mitochondrial and glycolysis stress test) were generated using the Seahorse XF96. Radiosensitivity was investigated by performing clonogenic survival assays after exposing cells to different irradiation doses.
Results: For the parental cell lines, the A549 cells had a higher mitochondrial ATP production, less spare OXPHOS capacity and more proton leak. 143B were more dependent on glucose metabolism and had the lowest glycolytic reserve capacity. The BEAS-2B cells showed an intermediate result for both assays. Different characteristics of a ρ^0 cell are changed compared to its parental cell. All ρ^0 cell lines showed reduced mitochondrial respiration, whereas increased glycolysis was observed with a lack of glycolytic reserve compared to the parental lines. The ρ^0 phenotype also resulted in a decreased proliferative capacity of these cells. Dose response curves showed that BEAS-2B ρ^0 cells were more radioresistant ($p<0.0001$) while 143B ρ^0 showed a more radiosensitive phenotype compared to the parental counterparts ($p<0.0007$). For the A549 cells no differences were found for radiosensitivity between parental and ρ^0 cell lines.
Conclusions: These findings suggest that different types of ρ^0 react differently upon irradiation. It has been suggested that the capacity to cope with metabolic stress determines the radiosensitivity of tumor cells and might be correlated to the metabolic profile of the parental cells. Therefore, we are currently investigating if varying ROS levels or basal ATP production of the cells drives these differences in radiosensitivity by e.g. influencing antioxidant defenses and if known OXPHOS inhibitors (e.g. rotenone, metformin) could potentially demonstrate the same effects.

Proffered Papers: Physics 9: Evaluation and mitigation strategies for intrafraction

OC-0545

Quantification of respiration-induced esophageal tumor motion using fiducial markers and 4D computed tomography

P. Jin[1], M.C.C.M. Hulshof[1], R. De Jong[1], J.E. Van Hooft[2], A. Bel[1], T. Alderliesten[1]
[1]*Academic Medical Center, Radiation Oncology, Amsterdam, The Netherlands*
[2]*Academic Medical Center, Gastroenterology & Hepatology, Amsterdam, The Netherlands*

Purpose/Objective: Respiration-induced tumor motion is an important source of geometric uncertainty in radiotherapy for (gastro-) esophageal cancer. However, it is difficult to quantify this motion particularly in the cranio-caudal (CC) direction due to the limited soft tissue contrast on CT. In this study, we aimed at quantifying esophageal tumor motion relative to the bony anatomy using markers and 4DCT data.
Materials and Methods: Eighteen esophageal cancer patients underwent endoscopy-guided implantation of in total 65 markers, of 3 different types, at the cranial border, caudal border, and/or the center of the primary tumor. A 4DCT scan was acquired after marker implantation for all patients. Table 1 gives an overview of patient and marker characteristics. The 4DCT scans were reconstructed and sorted into 10 phases throughout a breathing cycle. Retrospectively, for each patient, the 1st phase (0%, the end of inhale) in the 4DCT was selected as the reference to which the 9 remaining phases were rigidly registered based on the vertebra. Then, markers were manually identified and classified into 3 groups based on their positions in the esophagus as measured from the incisors: proximal, mid and distal esophagus. Next, individual marker displacements in each phase relative to the reference positions were assessed in the left-right (LR), CC, anterior-posterior (AP) directions, and vector distance (3D).
Results: In total, 56 markers could be identified: 3, 13 and 40 markers in the proximal, mid, and distal esophagus, respectively (Table 1, Figure 1). Different types of markers showed no difference in visibility on 4DCT. Figure 1 shows the mean and standard deviation (SD) of the marker displacements relative to the reference in each breathing phase. Also the distribution of the maximum difference in marker position over the course of one breathing cycle in the LR, CC, and AP directions as well as in 3D is shown. For all 56 markers, the maximum difference in position (mean ± SD) was 3.0 ± 2.1, 6.0 ± 2.8, and 3.4 ± 2.0 mm in the LR, CC, and AP directions, respectively. Overall, displacements were significantly larger in the CC than in the LR and AP directions ($p<0.05$, Wilcoxon signed-rank test). However, for all 4 distally located markers in patient 13 distinct larger displacements in the LR than in the CC and AP directions were observed. Moreover, the 3D maximum difference in marker position was 2.9 ± 1.1 in the proximal, 3.6 ± 1.8 in the mid, and 8.6 ± 2.4 mm in the distal esophagus. In all 3 directions and in 3D, displacements of markers located in the distal esophagus were significantly larger than of markers in the proximal and mid esophagus ($p<0.05$, Wilcoxon rank-sum test).
Conclusions: Generally, respiration-induced motion is largest in the CC direction. However, the motion in the LR and AP directions cannot be neglected when the tumor is located in the distal esophagus. Hence, with clearly visible markers on 4DCT, the respiration-induced motion could be incorporated to individualize the safety margin, by for instance using an internal target volume, mid-ventilation, or breath-control technique.